Temperature and doping dependence of phonon lifetimes and decay pathways in GaN

Thomas Beechem and Samuel Graham

Citation: J. Appl. Phys. **103**, 093507 (2008); doi: 10.1063/1.2912819
View online: http://dx.doi.org/10.1063/1.2912819
View Table of Contents: http://jap.aip.org/resource/1/JAPIAU/v103/i9
Published by the American Institute of Physics.

Temperature and doping dependence of phonon lifetimes and decay pathways in GaN

Thomas Beechem and Samuel Graham[a)]
G. W. Woodruff School of Mechanical Engineering, Georgia Institute of Technology, 771 Ferst Dr. NE, Atlanta, Georgia 30332, USA

(Received 23 December 2007; accepted 26 February 2008; published online 2 May 2008)

The lifetimes of polar optical phonons are known to affect both the electrical and thermal performances of gallium nitride (GaN) based devices. Hence, understanding the dynamical behavior of these phonons in GaN is integral to the elucidation of carrier drift velocities, hot phonon effects, and temperature localization in these nitride semiconductors. To investigate this dynamic behavior, temperature dependent phonon lifetimes were acquired through utilization of the linewidth of the Raman response for GaN samples having various doping types and concentrations. The temperature dependent lifetimes of the four examined phonon modes were then correlated with the Klemens decay model modified to account for four-phonon processes to deduce the decomposition of the zone center phonons. A graphical method that maps this decomposition in the high symmetry directions of the Brillouin zone is also presented. From the variation in lifetime with free carrier concentration, dominant scattering mechanisms are subsequently found for each of four different phonon modes. It is observed that the phonon-carrier interaction directly determines the lifetimes of the polar optical $A1$ and $E1$(LO) modes, while the transverse modes into which these longitudinal phonons decay are independent of this interplay. These results indicate that temperature localization likely arises due to the continual emission and reabsorption between the LO phonon modes and the free carriers rather than the persistence of lattice/carrier interaction throughout the entirety of the energy cascade. © *2008 American Institute of Physics*. [DOI: 10.1063/1.2912819]

I. INTRODUCTION

Gallium nitride (GaN) is an attractive material for a host of microelectronic and optoelectronic applications due to both its inherent chemical stability and wide bandgap.[1,2] These attributes allow operation at high temperature, frequency, and electric fields, qualities which are desirable for implementation into power electronics and rf communications.[3] However, to improve these devices to allow for their mainstream adoption, significant technical challenges remain. Chief among these challenges is the mitigation of considerable self-heating through phonon-carrier interactions and subsequent hot spot formation, which was shown to degrade both performance and reliability.[4–6]

Phonon-carrier interactions arise due to the polar nature of the gallium nitride lattice itself and, in particular, the strong coupling between the free carriers and the longitudinal optical (LO) modes.[7] This interaction manifests itself upon application of an electric field, whereupon electrons are accelerated until their energy is sufficient to emit optical phonons. To maintain an equilibrium state, it is necessary that these emitted phonons decay at a rate equal to their creation. In actuality, the lifetime of the emitted phonons is over an order of magnitude longer than the characteristic emission time, which leads to a nonequilibrium distribution of these polar LO phonons.[8] The nonequilibrium distribution of these LO phonons, which are termed as "hot phonons," is deleterious as their presence was shown to significantly reduce electron drift velocity and, thus, overall device performance.[9,10] Only through efficient decay of these hot phonons into other phonon modes is this effect minimized and performance then maximized. Thus, the rate of this decay and the mechanisms by which it occurs are then of primal importance to the development of next generation devices.

Phonon decay is also pertinent from a thermal perspective as devices must efficiently dissipate heat to maintain operating temperatures typically required to be less than 200 °C.[11] To effectively dissipate this energy, optical phonon modes with a low group velocity must decay into acoustic modes with a high group velocity at a rate commensurate with the power supplied to the device.[12] When these phonon transformations do not occur with sufficient celerity, the temperature in the device will increase, leading to subsequent reductions in performance and reliability.[13,14]

The lifetimes of zone center optical phonons can be experimentally determined through a number of techniques, including steady state and time resolved Raman spectroscopy, as well as microwave noise measurements.[5,6,15] In using steady state Raman spectroscopy, the linewidth, Γ (full width at half maximum), of the Stokes peak can be directly correlated with the lifetime of the measured phonon through the energy-time uncertainty relation.[15,16] Time resolved Raman spectroscopy, on the other hand, does not rely on this relation but instead deduces the lifetime through examination of the decay in the temporal response of the anti-Stokes Raman signal.[17] In contrast to these optical techniques, the microwave noise procedure relies on an interaction between the phonon and the free carriers, thus, limiting its application to

a)Electronic mail: sgraham@gatech.edu.

only particular modes. This interaction allows for the creation of a simple energy balance, which when used in concert with measurements of the rate at which electrons gain and lose energy, allows for estimation of the phonon lifetime.[5,18]

Regardless of the technique employed, measuring the lifetimes of a particular mode at several temperatures allows for prediction of the phonon decay path through the use of perturbation theory. Knowledge of the decay pathway, in turn, gives insight into the entire lattice energy cascade and visualization of the energy "flow." Through careful examination of this flow, energy bottlenecks may be identified and future avenues for device improvement through phonon engineering are illuminated. By using standard Raman spectroscopy, previous studies identified these pathways for five different phonon modes in standard bulk samples of GaN having relatively low free carrier concentrations ($n < 10^{17}$ cm^{-3}).[19,20]

In the presence of a high free carrier concentration ($n > 5\times10^{17}$ cm^{-3}), however, the LO phonons become strongly coupled with the presence of plasmons, forming what is commonly referred to as a longitudinal optical phonon-plasmon (LPP) coupled mode.[21,22] Tsen *et al.*[6] used this coupled mode, in turn, to deduce the lifetime of the $A1$(LO) phonon and showed an inverse relationship between the rate of decay and the free carrier concentration. Due to this dependency, questions then arise as to the extent of free carrier interaction throughout the entirety of the energy cascade. In response, this study analyzes the decay of four-phonon modes in a series of GaN samples having carrier concentrations ranging from 3×10^{17} to 1.24×10^{18} cm^{-3} at temperatures varied from 23–300 °C. By incorporation of this method, the lifetime, decay pathways, and carrier dependences will be enumerated for each of the modes, thus offering insight into relevant energy transfer mechanisms in GaN based devices.

II. EXPERIMENTAL

A series of gallium nitride wafers was produced through the use of a metal organic chemical vapor deposition. Three different wurtzite GaN samples were examined in this study, namely, *n*-type GaN (*n*GaN) acquired through Si infiltration, *p*-type GaN(*p*GaN) attained by utilizing a Mg implantation procedure, and bulk type GaN (GaN). Through room temperature analysis of the spectral profiles of the LPP modes, it was found that the free carrier concentration for the *n*-type, *p*-type, and bulk GaN samples were 1.2×10^{18}, 6.4×10^{17}, and 3×10^{17} cm^{-3}, respectively.[23] In addition, it is of note that the doped regions described thus far rest directly on top of an undoped GaN buffer layer to assure the highest quality lattice structures. Further details regarding both the growth and initial characterization of the GaN samples studied here can be found in Refs. 24–26.

Phonon lifetime measurements were carried out by using a Renishaw InVia Raman system. The system utilized a 488 nm Ar^+ laser in the 180° backscattering mode through a 50 × objective. In this region of the spectrum, GaN is transparent and, as such, the probing radiation interacts with both the doped and the undoped GaN buffer layers. The acquired signals will, thus, have contributions stemming from each region. However, as this buffer layer is consistent between each of the differently doped samples, qualitative comparisons between the specimens remain valid. With this understanding, samples were measured at typical device operating temperatures ranging from 23–300 °C using a Linkam TS-1200 heated stage along both the *c* and *a* axes in order to capture four of the Raman active modes [A_1(LO), A_1(TO), E_1(LO), and E_2^{high}]. In the backscattering arrangement, the $E1$(LO) mode is forbidden and, as such, the actual measured values are that of the quasi-LO or Q(LO) mode. This Q(LO) mode, however, was used to directly estimate the lifetime of the $E1$(LO) mode in the work of Song *et al.*[20] and will likewise be utilized here.

Of the four modes investigated, the E_2^{high} mode is the only nonpolar phonon mode and will be used for comparison to the behavior of the other polar optical phonon modes. This same mode is also used as a built-in temperature sensor to verify the sample temperature during the experiments by using basic Raman thermometry techniques.[27] For each temperature and phonon mode, at least 20 acquisitions of the Raman signal were acquired, resulting in uncertainties that were no more than ±3.7% and most often less than ±1% of the measured lifetime value.

III. RESULTS

A. Temperature dependence of the phonon lifetimes

The measured Raman linewidths are a convolution of effects stemming from both the spectrometer-induced broadening and the actual Lorentzian vibrational distribution of the phonons in the crystal lattice. It is typically assumed that the spectrometer imposes a Gaussian response on the signal from the crystal lattice that is itself Lorentzian in character. Thus, the Raman spectrum data are fitted by using the mathematical convolution of these functions known as the Voigt profile.[28] Consequently, the "as acquired" measured linewidth cannot be directly used to obtain the phonon lifetime as it has effects evolving from both the crystal and the response function of the spectrometer.

To obtain the actual crystal lattice linewidth, the Voigt profile is deconvoluted by using Posener's tables with knowledge of the Gaussian response function of the spectrometer.[29,30] The Gaussian response function can be determined through calibration with plasma lines of an extended neon source at varying slit widths. The lifetime is subsequently calculated by using the energy-time uncertainty relation with the true linewidth, as shown by:[31]

$$\tau = \frac{\hbar}{\Gamma}, \tag{1}$$

where τ is the lifetime in picosecond, $\hbar$ is the modified Planck constant (5.3 cm^{-1} ps), and Γ is the true crystal linewidth.

By using this deconvolution procedure, phonon lifetimes were examined for the four-phonon modes in each of the three samples investigated. Quantitatively, it was found that the room temperature lifetimes of the E_2^{high}, $A1$(LO),

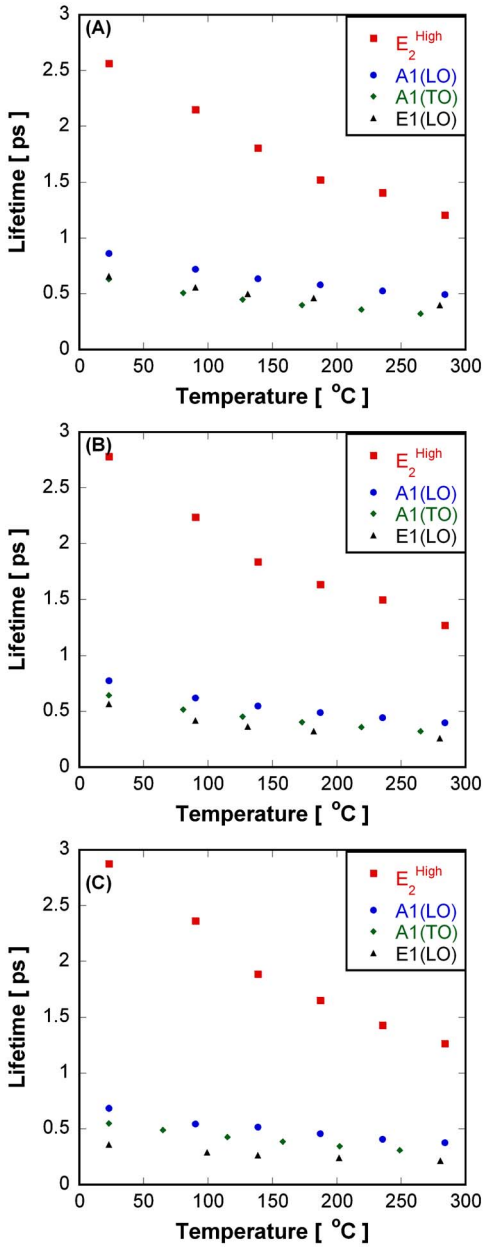

FIG. 1. (Color online) Phonon lifetime vs temperature for each mode examined in (a) bulk GaN, (b) *p*-type GaN, and (c) *n*-type GaN. Analysis of the temperature dependence of these lifetimes can be used to identify the decay pathways of the phonon modes.

$A1$(TO), and $E1$(LO) modes were 2.56, 0.86, 0.63, and 0.66 ps, respectively, for the bulk GaN sample. These lifetimes correlate well with the recent work of Song *et al.*,[20] who reported similar values of 2.5, 0.75, 0.5, and 0.58 ps for these same respective modes for bulk GaN at room temperature.

Figure 1 shows the temperature dependence of the lifetimes for each of the four-phonon modes for the bulk, *p*-doped, and *n*-doped GaN samples. From Fig. 1, it is seen that for all samples, an increase in temperature is accompanied by an associated decrease in phonon lifetime. This decrease occurs as the rate of phonon-phonon scattering increases with temperature due to the associated increase in the phonon thermal occupancy and, hence, their interaction. Yet despite this qualitative uniformity, there exist significant

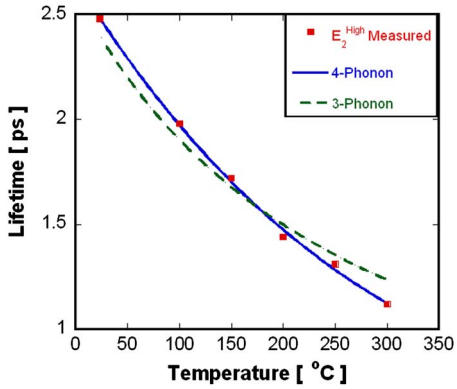

FIG. 2. (Color online) Measured E_2^{high} mode for bulk GaN fitted by accounting for only three-phonon processes (dashed line) and by using both three- and four-phonon processes (solid line). It can be seen that four-phonon processes are quite relevant at the temperatures examined here.

quantitative differences between the lifetime values for many of the modes. This is exemplified for the $A1$(LO) mode, where at room temperature, the lifetime is seen to decrease from 0.86 ps with a carrier concentration of 3.1×10^{17} cm^{-3} to 0.68 ps at a concentration of 1.24×10^{18} cm^{-3}. The underlying cause for this discrepancy, whether it be changes in the lattice due to the doping procedure or actual phonon-carrier interaction, cannot be enumerated solely based on the differences between these lifetime values. Rather, it is necessary to compare the decay processes for each of the different samples to identify the underlying causes for the variation in the lifetimes. Consequently, Secs. III B and III D will examine the decay pathways for each mode to determine the lifetime's dependency on free carrier concentration.

B. E_2^{high} phonon decay channels and carrier dependency

By using the temperature dependent phonon lifetimes seen in Fig. 1, it is possible to determine the phonon decay pathways in the Brillouin zone. By assuming that each optical phonon dissipates into two phonons in a so-called three-phonon process, Klemens[32] obtained the following relation for the linewidth of a crystal based upon perturbation theory:

$$\Gamma_3(T) = \Gamma_D + \Gamma_0\left(1 + \sum_{i=1}^{2} \frac{1}{e^{(x_i)} - 1}\right), \tag{2}$$

where Γ_0 and Γ_D are fitting parameters that represent the linewidth at 0 K and $x_i = \hbar\omega_i / k_B T$, where k_B is Boltzmann's constant, T is the temperature in Kelvin, $\hbar$ is, again, modified Planck's constant only this time in standard units of J/s, and ω_i is the frequency of the resulting phonon after the scattering process. Due to conservation of energy, the following relation must be satisfied: $\omega_0 = \omega_1 + \omega_2$. By using Eq. (2), the temperature dependent linewidths were fitted for the E_2^{high} mode assuming a symmetric decay process ($\omega_0/2 = \omega_1 = \omega_2 = 284$ cm^{-1}) and then transformed to a lifetime value per Eq. (1). As seen in Fig. 2 for the bulk GaN sample, it was found that the resulting curve did not correlate well with the measured lifetime values. Consequently, it is necessary to ac-

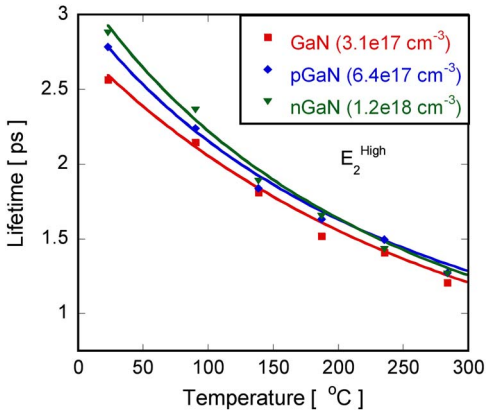

FIG. 3. (Color online) Phonon lifetime vs temperature for the E_2^{high} mode of bulk, *p*-type, and *n*-type GaN. The symbols are the measured values, while the lines represent the fitting obtained by using Eq. (3). Notice that at higher temperatures, the lifetimes converge, indicating the dominance of phonon-phonon scattering and a lack of phonon-carrier interaction.

count for more complex and possibly asymmetric decay mechanisms.

Balkanski *et al.*[33] accounted for these complex decay mechanisms through modification of Klemens' original model through consideration of both three- and four-phonon processes. In a four-phonon process, the decay of the phonon is assumed to occur into three separate phonons and Eq. (2) is revised into the form shown below,

$$\Gamma_4(T) = \Gamma_3(T) + \Gamma_1\left[1 + \sum_{i=3}^{5} \frac{1}{e^{(x_i)} - 1} + \sum_{i=3}^{5} \frac{1}{(e^{(x_i)} - 1)^2}\right], \tag{3}$$

where Γ_1 is an additional fitting parameter representing a portion of the linewidth at 0 K. By incorporating this fitting procedure and assuming equivalent decay for the four-phonon process ($\omega_3 = \omega_4 = \omega_5 = \omega_0/3$), Eq. (3) was found to have excellent correlation with the data for the E_2^{high} mode, as seen in Fig. 2. As this same fitting model was also capable of predicting each of the differently doped sample's responses (Fig. 3), it can be reasoned that the phonon decomposition mechanisms are identical despite the changes in free carrier concentration.

The actual path of decomposition may be identified through examination of the Brillouin zone of GaN as in any scattering event energy must be conserved, while phonon momentum must similarly be preserved within a reciprocal lattice vector. To examine the phonon momentum (energy was conserved as part of the fitting procedure), it must be noted that due to the wavevector of the incident light, it is only those phonons near the Gamma point that are measured during the acquisition of a first order Raman spectrum.[23] Consequently, in the assumption of a symmetric three-phonon decay process, conservation of the phonon momentum stipulates that the resulting phonons must have wavevectors opposite of each other with respect to the Gamma point of the Brillouin zone. This fact remains valid even after an umklapp process as with the addition or subtraction of a reciprocal lattice vector, the resulting phonon has an identical wavevector, although in an adjacent zone.

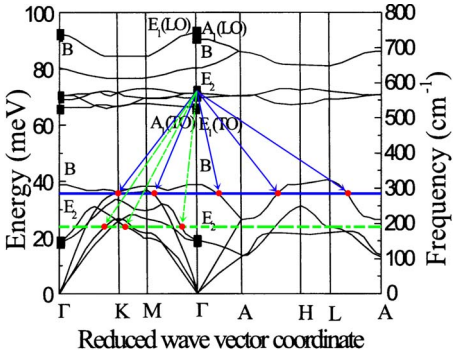

FIG. 4. (Color online) Dispersion curve of wurtzite GaN as reported by Siegle *et al.* (Ref. 41). The decay of the E_2^{high} phonon is shown to occur via a combination of symmetric three- and four-phonon decays. Notice the points (dots) on the curve satisfy the momentum criterion, indicating an allowed scattering event.

In a similar manner, momentum conservation of the phonons necessitates that in a four-phonon process, the sum of the three resulting phonon wavevectors must be equal to 0. As there is a relation between energy (frequency) and phonon momentum (wavevector) via the lattice dispersion curve, only certain transformations will be allowed. Thus, by examining the scattering processes with respect to the dispersion curve, one can easily assure the viability of a scattering mechanism while simultaneously tracing the decay pathway of the phonon.

Previously, it was shown that suitable fitting of the experimental lifetime data for the E_2^{high} mode was obtained by assuming a symmetric decay process wherein the phonon decays into two phonons of energy $\omega_0/2$ and a four-phonon process by which three phonons of energy $\omega_0/3$ result. If the dispersion curve, as seen in Fig. 4, is then examined at these resulting energies (the solid 284 cm^{-1} and dashed 189 cm^{-1} lines), decay can take place only if points on the dispersion curve are present that also satisfy the momentum criterion. For example, the momentum criterion is satisfied for symmetric decay at points on the dispersion that intersect the constant $\omega_0/2$ energy line as two resulting phonons of opposite wavevector at this intersection will result. Similarly, viability of the four-phonon process can be assured if intersection between the $\omega_0/3$ energy line and the dispersion curve occurs at a set of three locations such that the resulting wavevectors sum to 0. In Fig. 4, the solid and dashed arrows identify such locations along the constant $\omega_0/2$ and $\omega_0/3$ energy lines that satisfy these conditions for both the three- and the four-phonon processes, respectively. As a consequence, the hypothesized decay model is then validated while simultaneously illustrating possible avenues for the decomposition of the E_2^{high} mode. Note that as the dispersion only gives information with regards to the directions of high symmetry and not the entire Brillouin zone, additional scattering pathways will no doubt be available. Thus, Fig. 4 gives possible, rather than definitive pathways. Yet even with knowledge of these possible decay routes, a preliminary picture of the energy cascade in GaN begins to form and the dominant cause of scattering can be identified through comparison of the lifetimes of the differently doped samples.

The lifetime of a phonon is limited by interactions with boundaries, defects, free carriers, and other phonons. If these interactions take place independent of one another, an assumption that may not remain strictly valid at high free carrier concentrations but is often employed to analyze GaN carrier transport nonetheless, Matthiessen's rule allows for the scattering as a whole to be examined through analysis of the individual scattering sources themselves.[34–36] During the Raman measurement, a large set of individual scattering events is probed and the resulting lifetime is an average composed of contributions from each of these scattering sources. This average is weighted toward those events occurring most often and, hence, the scattering source with the greatest strength. In general, the combined strength of a scattering source is population dependent, depending on defect density, phonon population, carrier population, etc. Differences in the measured lifetimes then arise due to disparities in the populations of the scattering sources themselves. Thus, by understanding the temperature dependent populations of the scattering sources, it becomes possible to identify the dominant scattering mechanism in each of the differently doped samples.

As GaN has a stable crystal arrangement, the microstructure may be assumed to remain static during the measurements and, hence, so too the number of defects. Thus, with an increase in temperature, the number of scattering events arising from the presence of defects will remain largely constant. In contrast, the number of both phonon-phonon and phonon-carrier scattering events will change with temperature as the number of these species available for interaction varies due to their temperature dependent Bose–Einstein and Fermi–Dirac distributions, respectively. Therefore, with an increase in temperature and a concomitant increase in the number of phonons and free carriers, the measured lifetime will become ever more weighted to the effect of these species rather than those of the microstructure. Consequently, comparison of the phonon lifetimes at higher temperatures between each of the doped samples allows for the effects of phonon and carrier scattering to be isolated from those stemming from the microstructure.

Separation of the carrier and phonon effects may then occur by recognizing that each of the differently doped samples remains in a GaN wurtzite crystal arrangement and, as such, displays a nearly identical dispersion. With similar dispersions, the levels of phonon-phonon scattering will be practically equivalent between the specimens. In contrast, the numbers of carriers and, hence, the levels of carrier scattering will be different between the samples owing to the variance in doping concentration. As the value of the lifetime is intrinsically tied to the population of the scatterers, similarities in the measured lifetimes may evolve only through a dominant source common to all samples. Only phonon-phonon scattering is similar in each of the specimens and, thus, a convergence in the value of the lifetimes indicates a dominance in this form of scattering and an associated independence of carrier scattering. By using this deductive procedure, similarities in the lattice scattering are seen in Fig. 3, wherein the lifetimes of the E_2^{high} mode converge to a common value of ~ 1.25 ps near 300 °C, indicating a prevalence of phonon-phonon scattering and, as expected, an independence of carrier interaction. At lower temperatures, meanwhile, the lifetime widely varies between samples as microstructural differences arising from the doping procedure become an ever more dominant scattering source.

C. *A*1(LO) and *E*1(LO) phonon decay channels and carrier dependency

At high free carrier concentration, coupling occurs between the LO modes and plasmons creating a LPP coupled mode. This LPP mode has a spectral shape dependent on the frequency of the free carriers and was used as a complement to Hall measurements in the determination of free carrier concentration.[21,37] Recently, Tsen *et al.*[6] used this LPP mode to measure the lifetime of the $A1$(LO) phonon, by assuming equivalent durations for both the coupled and vibrational modes. By using this same assumption, it is then possible to examine the decomposition processes of the $A1$(LO) and $E1$(LO) phonons. To determine these processes, the modified Klemens decay model that uses the Ridley decomposition channel, which is presented in Eq. (3), was utilized to simulate the temperature dependent lifetime response for both the $A1$(LO) and $E1$(LO) modes.

Unlike the E_2^{high} mode, high energy $A1$(LO) and $E1$(LO) lifetimes cannot be modeled by using a symmetric phonon decay process since $\omega_0/2$ occurs in a large phonon bandgap of the dispersion curve. For the $A1$(LO) mode, it was both theoretically postulated by Ridley[38] and experimentally verified by Tsen *et al.*[39] that an asymmetric three-phonon process is the dominant decay pathway, whereby the LO phonon decomposes into a TO and longitudinal acoustic mode. By assuming this asymmetric decomposition for the three-phonon process in Eq. (3), while making no other assumptions for the four-phonon process, the temperature dependence of the $A1$(LO) and $E1$(LO) modes was modeled for each of the different samples with excellent correlation, as seen in Fig. 5. From these fitted models, the ratio of Γ_0/Γ_1 was found to be >50 for each case, illustrating the clear dominance of the three-phonon decay process. The pathways for these transformations are shown in Fig. 6, wherein it is evident that the decay into the TO mode at a wave number of ~ 530 cm^{-1}, indeed, occurs. In light of these results, it then becomes apparent that the avenue for decay of the phonons themselves is independent of carrier concentration.

Due to an intense Fröhlich interaction, the higher energy optical modes heavily interact with free carriers.[37,40] Recently, this was experimentally shown as under nonequilibrium fields, the phonon lifetime of the $A1$(LO) mode is observed to inversely vary with the free carrier concentration.[5,6] In this study, however, the incident laser light is below the bandgap of the GaN and the equilibrium response of the crystal is probed instead. Yet despite this significant difference between the conditions in this study and those of previous studies, a similar trend for the $A1$(LO), as well as the $E1$(LO) mode, is found as the lifetime is seen to decrease across all temperatures with an increase in free carrier concentration (Fig. 5). Quantitatively, this trend is exhibited at room temperature at which the lifetimes of the $A1$(LO) mode

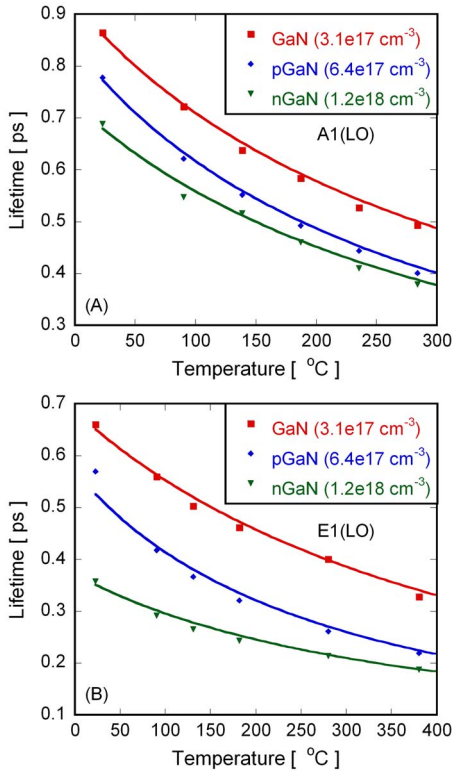

FIG. 5. (Color online) Lifetimes of the (a) $A1(LO)$ and (b) $E1(LO)$ modes as a function of temperature. Unlike the E_2^{high} mode, the lifetimes of the LO modes remain distinct across the entirety of the examined temperature range, indicating interactions with the free carriers. As expected, the lifetimes decrease with an increase in free carrier concentration.

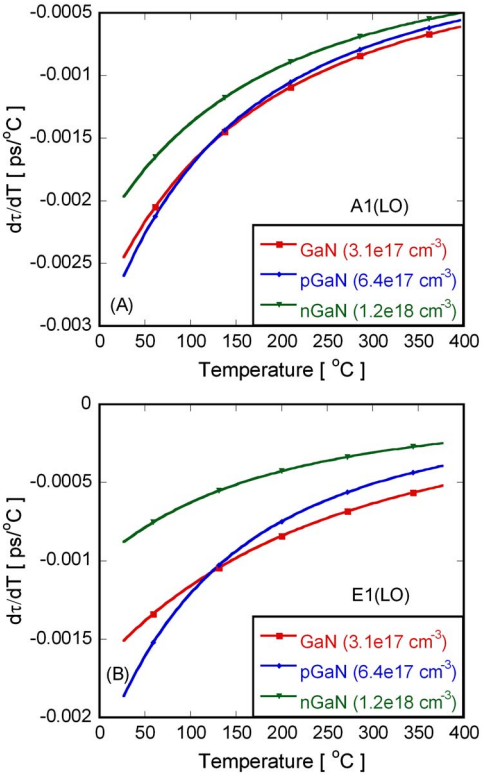

FIG. 7. (Color online) Rate of change in the lifetime of the (a) $A1(LO)$ and (b) $E1(LO)$ modes with respect to temperature. Utilizing the rate of change isolates the source of scattering to only other phonons and free carriers. As the phonon-phonon scattering is equivalent between each of the samples, the discrepancy in the rate of change indicates that differences in the lifetime values may be attributed to direct phonon-carrier interaction.

were found to vary between 0.86 and 0.69 ps across a carrier concentration range of $3.1\times10^{17}-1.2\times10^{18}$ cm^{-3}. These values are within the lifetime range of 2–0.51 ps recently reported by Tsen *et al.*[6] for GaN in a similar concentration regime.

The dependency of the lifetime on doping concentration occurs due to a direct interaction of the phonons with the carriers rather than differences in the microstructure arising from to the doping procedures themselves. While the doping process does induce distortion of the lattice and, hence, strain

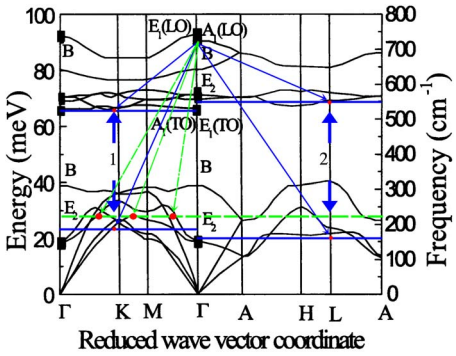

FIG. 6. (Color online) Dispersion curve of wurtzite GaN as reported by Siegle *et al.* (Ref. 41). The asymmetric decay of the LO phonons occurs via decomposition into a TO mode. Notice that although the four-phonon process may occur via the dashed line, three-phonon processes dominate in the determination of the lifetime for these modes. Note that, although only the $A1(LO)$ pathways are shown, the pathways for the $E1(LO)$ mode are extremely similar.

fields that affect phonon scattering, these microstructural effects are not the dominant scattering source. Rather, the carriers themselves weigh most heavily on the scattering of the LO modes. This is first indicated upon investigation of Fig. 5, wherein the lifetimes do not converge at higher temperatures. The lack of convergence indicates that phonon-phonon scattering is not the dominant mechanism as was the case for the nonpolar E_2^{high} mode. Hence, an additional source of scattering either in the form of microstructural differences or direct carrier/phonon interaction must be present even at these higher temperatures.

To ascertain the nature of this additional scattering source, it is useful to examine the rate of change in the lifetime with respect to temperature ($\partial\tau/\partial T$). Utilizing the derivative is pertinent, allowing for the removal of microstructural effects as, again, this scattering source remains largely constant with temperature. Consequently, through examination of the derivative, only the effects of phonon-phonon and phonon-carrier scatterings are investigated. Hence, due to the sample's common dispersion, a convergence of the lifetime's derivative with respect to temperature indicates that the phonon-phonon scattering is dominant and, thus, differences in the actual lifetime evolve from microstructural differences. Upon investigation of Fig. 7, however, it is seen that for each LO mode, the rate of change in the lifetime remains distinct at all temperatures. This result indicates that the dominant source of scattering varies in its temperature de-

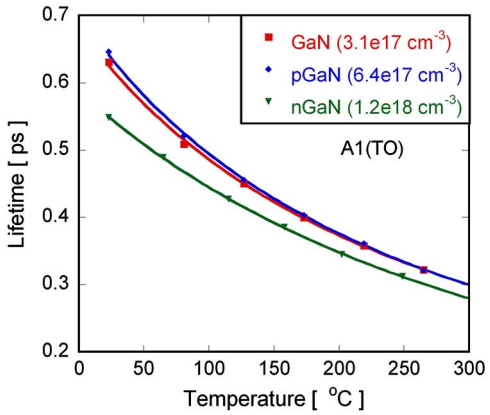

FIG. 8. (Color online) Lifetime vs temperature for the $A1(TO)$ mode. Although convergence is seen at higher temperature for the lower doped samples (GaN and *p*GaN), the higher doped *n*GaN specimen has a lifetime clearly distinct from these other two specimens, raising suspicions that carriers may interact with this mode.

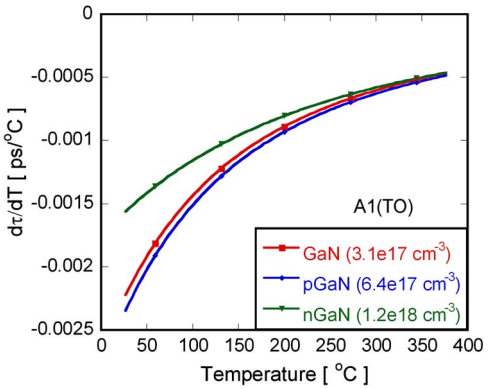

FIG. 10. (Color online) Rate of change in the lifetime of the $A1(TO)$ and with respect to temperature. Convergence in this rate of change is seen for each of the differently doped samples, indicating the absence of any phonon-carrier interaction. Consequently, differences in the lifetimes arise due to interaction with the microstructure.

pendent population between each of the specimens examined. It may then be deduced that the carriers themselves directly interact with the LO modes.

D. *A*1(TO) phonon decay channels and carrier dependency

Charge carriers in GaN strongly interact with the LO optical modes and, thus, several researchers have concentrated on the lifetimes of these polar optical phonons. However, as shown in Sec. III C, the LO modes undergo asymmetric decay into transverse optical (TO) modes. Thus, understanding the lifetimes and decay mechanisms of these TO modes is also necessary to elucidate the entirety of the phonon energy cascade into acoustic modes. To this end, the temperature dependence of the $A1(TO)$ mode was fitted by using Eq. (3), as shown in Fig. 8. For each sample, excellent correlation between the model and data is achieved assuming symmetric decay for the three-phonon process ($\omega_0/2 \approx 266\ \mathrm{cm}^{-1}$) along with an associated value of $\omega_0/3$ utilized for the four-phonon process. This decay pathway is viable as indicated in Fig. 9 by the points of intersection annotated along the constant energy lines of 266 and 177 cm^{-1} corresponding to the three- and four-phonon processes, respectively.

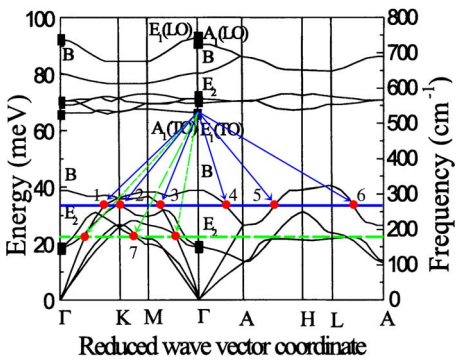

FIG. 9. (Color online) Dispersion curve of wurtzite GaN as reported by Siegle *et al.* (Ref. 41). Decay for the $A1(TO)$ occurs via both three-phonon processes (solid line) and four-phonon processes (dashed line).

Further examination of Fig. 8 displays convergence of the lifetimes at higher temperatures for the lower doped samples (GaN and *p*GaN), while the lifetime of *n*GaN specimen is continually lower. This difference with doping does not arise due to a direct interaction of the phonon with the carrier, however, but rather as a consequence in heavier scattering with the microstructure in the *n*GaN sample. Examination of Fig. 10 verifies this assertion as the rate of change in the lifetime with temperature converges for each of the samples. This indicates that the temperature dependent scattering sources are similar in each of the samples and, thus, carrier interaction does not occur. Therefore, carrier interaction does not permeate through the entirety of the energy cascade. Instead, energy flows regardless of carrier concentration once decay from the higher energy LO modes is accomplished.

IV. CONCLUSION

By using the energy-time uncertainty relation, phonon lifetimes were measured for four different optical modes in a series of gallium nitride samples, each having a different free carrier concentration. By measuring the lifetimes across the typical operating temperature spectrum for GaN devices, decay mechanisms and pathways for each of the different modes were deduced. Lower energy modes were found to decay via a combination of symmetric three- and four-phonon processes. In contrast, the higher energy LO modes primarily decomposed via asymmetric three-phonon Ridley decay. Through the use of previously determined dispersion relations, a graphical technique accounting for both the conservation of energy and phonon momentum allows for visualization of the entire energy cascade. The effect of free carrier concentration on phonon decay was then examined for each of the four modes through an analysis of both the lifetime and the rate of change in lifetime with respect to temperature. Through this analysis, it was found that only the high energy LO modes directly interact with the free carriers, while the modes into which the LO modes decay are independent of their presence. Consequently, upon decomposition of a LO mode, energy propagates independently of the

presence of carriers. Therefore, the most significant bottleneck to energy dissipation in GaN devices occurs as a result of the inefficient decay of the LO modes into lower energy lattice vibrations. Future studies should then focus on limiting the ability of free carriers to reabsorb these polar modes to maximize energy transfer, thereby limiting the likelihood of hot spot formation.

ACKNOWLEDGMENTS

Support for this research was provided by the NSF CAREER Award No. CTS-0448795 and the Air Force Research Laboratory. Special thanks to Professor Russ Dupuis, who graciously supplied each of the GaN samples used in this study.

[1]A. Link and K. Bitzer, J. Appl. Phys. **86**, 6256 (1999).
[2]C. H. Oxley, M. J. Uren, A. Coates, and D. G. Hayes, IEEE Trans. Electron Devices **53**, 565 (2006).
[3]A. Christensen, S. Graham, and W. Doolittle, IEEE Trans. Electron Devices **52**, 1683 (2005).
[4]M. Kuball, J. W. Pomeroy, S. Rajasingam, A. Sarua, M. J. Uren, T. Martin, A. Lell, and V. Harle, Phys. Status Solidi A **202**, 824 (2005).
[5]A. Matulionis, Phys. Status Solidi A **203**, 2313 (2006).
[6]K. T. Tsen, J. G. Kiang, D. K. Ferry, and H. Morkoc, Appl. Phys. Lett. **89**, 112111 (2006).
[7]M. Stroscio and M. Dutta, *Phonons in Nanostructures* (Cambridge University Press, Cambridge, 2001).
[8]K. Wang, J. Simon, N. Goel, and D. Jena, Appl. Phys. Lett. **88**, 022103 (2006).
[9]A. Matulionis, J. Liberis, L. Ardaravicius, L. F. Eastman, J. R. Shealy, and A. Vertiatchikh, Semicond. Sci. Technol. **19**, S421 (2004).
[10]B. K. Ridley, W. J. Schaff, and L. F. Eastman, J. Appl. Phys. **96**, 1499 (2004).
[11]S. Singhal, T. Li, A. Chaudhari, A. W. Hanson, R. Therrien, J. W. Johnson, W. Nagy, J. Marquart, P. Rajagopal, J. C. Roberts, E. L. Piner, I. C. Kizilyalli, and K. J. Linthicum, Microelectron. Reliab. **46**, 1247 (2006).
[12]K. Kyhm, R. A. Taylor, and N. J. Cain, J. Korean Phys. Soc. **47**, S356 (2005).
[13]H. Kim, V. Tilak, B. M. Green, J. A. Smart, W. J. Schaff, J. R. Shealy, and L. F. Eastman, Phys. Status Solidi A **188**, 203 (2001).
[14]M. Meneghini, L. Trevisanello, G. Meneghesso, E. Zanoni, F. Rossi, M. Pavesi, U. Zehnder, and U. Strauss, Superlattices Microstruct. **40**, 405 (2006).
[15]L. Bergman, D. Alexson, P. Murphy, J. Nemanich, M. Dutta, M. Stroscio, C. Balkas, H. Shin, and R. Davis, Phys. Rev. B **59**, 12977 (1999).
[16]M. Kuball, J. M. Hayes, S. Ying, and J. H. Edgar, Appl. Phys. Lett. **77**, 1958 (2000).
[17]K. T. Tsen, R. P. Joshi, D. K. Ferry, A. Botchkarev, B. Sverdlov, A. Salvador, and H. Morkoc, Appl. Phys. Lett. **68**, 2990 (1996).
[18]A. Matulionis, J. Liberis, I. Matulionienė, M. Ramonas, L. F. Eastman, J. R. Shealy, V. Tilak, and A. Vertiatchikh, Phys. Rev. B **68**, 035338 (2003).
[19]Z. C. Feng, Opt. Eng. **41**, 2022 (2002).
[20]D. Y. Song, S. A. Nikishin, M. Holtz, V. Soukhoveev, A. Usikov, and V. Dmitriev, J. Appl. Phys. **101**, 053535 (2007).
[21]F. Demangeot, J. Frandon, M. A. Renucci, C. Meny, O. Briot, and R. L. Aulombard, J. Appl. Phys. **82**, 1305 (1997).
[22]T. Kozawa, T. Kachi, H. Kano, H. Nagase, N. Koide, and K. Manabe, J. Appl. Phys. **77**, 4389 (1995).
[23]H. Harima, J. Phys.: Condens. Matter **14**, R967 (2002).
[24]C. J. Eiting, P. A. Grudowski, and R. D. Dupuis, Electron. Lett. **33**, 1987 (1997).
[25]K. Shiojima, J. M. Woodall, C. J. Eiting, P. A. Grudowski, and R. D. Dupuis, J. Vac. Sci. Technol. B **17**, 2030 (1999).
[26]J. C. Carrano, T. Li, P. A. Grudowski, C. J. Eiting, R. D. Dupuis, and J. C. Campbell, J. Appl. Phys. **83**, 6148 (1998).
[27]T. Beechem and S. Graham, in *BioNanoFluidic MEMS*, edited by P. Hesketh (Springer, New York, 2007), p. 375.
[28]B. H. Armstrong, J. Quant. Spectrosc. Radiat. Transf. **7**, 61 (1967).
[29]J. W. Pomeroy, M. Kuball, H. Lu, W. J. Schaff, X. Wang, and A. Yoshikawa, Appl. Phys. Lett. **86**, 223501 (2005).
[30]D. Posener, Aust. J. Phys. **12**, 184 (1959).
[31]B. D. Bartolo, *Optical Interactions in Solids* (Wiley, New York, 1968).
[32]P. G. Klemens, Phys. Rev. **148**, 845 (1966).
[33]M. Balkanski, R. F. Wallis, and E. Haro, Phys. Rev. B **28**, 1928 (1983).
[34]S. Gokden, R. Baran, N. Balkan, and S. Mazzucato, Physica E (Amsterdam) **24**, 249 (2004).
[35]C. E. Martinez, N. M. Stanton, A. J. Kent, M. L. Williams, I. Harrison, H. Tang, J. B. Webb, and J. A. Bardwell, Semicond. Sci. Technol. **21**, 1580 (2006).
[36]B. K. Ridley, B. E. Foutz, and L. F. Eastman, Phys. Rev. B **61**, 16862 (2000).
[37]T. Kozawa, T. Kachi, H. Kano, Y. Taga, M. Hashimoto, N. Koide, and K. Manabe, J. Appl. Phys. **75**, 1098 (1994).
[38]B. K. Ridley, J. Phys.: Condens. Matter **8**, L511 (1996).
[39]K. T. Tsen, D. K. Ferry, A. Botchkarev, B. Sverdlov, A. Salvador, and H. Morkoc, Appl. Phys. Lett. **72**, 2132 (1998).
[40]M. Kuball, Surf. Interface Anal. **31**, 987 (2001).
[41]H. Siegle, G. Kaczmarczyk, L. Filippidis, A. P. Litvinchuk, A. Hoffmann, and C. Thomsen, Phys. Rev. B **55**, 7000 (1997).